We thank Drs H. Patashnick and Z. E. Switkowski for useful discussion.

L. J. LANZEROTTI
W. L. BROWN
J. M. POATE
W. M. AUGUSTYNIAK

Bell Laboratories,
Murray Hill, New Jersey 07974

Received 5 December 1977; accepted 20 January 1978.

1. Bertaux, J. L. & Blamont, J. E. *Nature* **262,** 263 (1976).
2. Whipple, F. L. *Astrophys. J.* **111,** 375 (1950).
3. Delsemme, A. H. & Wenger, A. *Planet. Space Sci.* **18,** 709 (1970).
4. Levy, E. H. & Jokipii, J. R. *Nature* **264,** (1976).
5. Patashnick, H. & Rupprecht, G. *Astrophys. J.* **197,** L79 (1975).
6. Patashnick, H. & Rupprecht, G. *Icarus* **30,** 402 (1977).
7. Brown, W. L., Lanzerotti, L. J., Poate, J. M. & Augustyniak, W. M. *Phys. Rev. Lett.* (in the press).
8. Sigmund, P. *Phys. Rev.* **184,** 383 (1969).
9. Lanzerotti, L. J. & Maclennan, C. G. *J. geophys. Res.* **78,** 3935 (1973).
10. Siscoe, G. L. & Mukherjee, N. R. *J. geophys. Res.* **77,** 6042 (1972).
11. Fisk, L. A., Kozlovsky, B. & Ramaty, R. *Astrophys. J.* **190,** L35 (1974).
12. Sarris, E. T. & Van Allen, J. A. *J. geophys. Res.* **79,** 4157 (1974).
13. Fisk, L. A. *J. geophys. Res.* **81,** 4633 (1976).
14. McDonald, F. B., Teegarden, B. J., Trainor, J. H. & Webber, W. R. *Astrophys. J.* **187,** L105 (1974).
15. Watson, W. D. & Salpeter, E. E. *Astrophys. J.* **174,** 321 (1972).
16. Aannestad, P. A. & Purcell, E. M. *Ann. Rev. Astr. Astrophys.* **11,** 309 (1973).
17. Watson, W. D. *Revs Mod. Phys.* **48,** 513 (1976).
18. Aannestad, P. A. *Astrophys. J. Suppl. Ser.* **25,** 223 (1973).
19. Wickramasinghe, N. C. & Williams, D. A. *Observatory* **88,** 272 (1968).
20. Daube, M. E., Augustyniak, W. M., Brown, W. L., Lanzerotti, L. J. & Poate, J. M. (in preparation).

Nucleation and growth of porous anodic films on aluminium

POROUS anodic films on aluminium are of considerable interest, not only because of their important practical uses in architecture and industry but also because of their novel regular morphology. The simple explanation involving field-assisted dissolution[1,2] has now been extended and an additional mechanism involving direct loss of Al^{3+} ions to solution has been proposed[3]. Ultramicrotomy[4] and ion beam thinning[5] of films, together with transmission electron microscopy and secondary ion mass spectrometry, have provided greater information on the film morphology and composition. Here we outline some of the more significant findings relating to the large-featured, regular films formed in phosphoric acid.

The initial, non-uniform growth of the anodic films formed in phosphoric acid at constant current density on aluminium (electropolished in a perchloric acid–ethanol mixture) is shown in Fig. 1. The micrographs show development of locally thicker film material to form approximately hexagonal cells (Fig. 1*a*, *b*). The cellular appearance is identical to that present on the metal surface after electropolishing and shows a similar metal grain orientation dependence. The thicker film material develops above ridges of metal initially present at the boundaries of the cells introduced by electropolishing. Formation of films, in nominally similar conditions, or substrates of a differently prepared but controlled surface cellular appearance (produced by forming a steady-state porous anodic film and dissolving the film in chromic/phosphoric acids to leave the scalloped substrate) confirms the preferential growth of material above the boundaries (Fig. 2). Likewise, where metal preparation is by etching, which produces a cellular network on the aluminium surface, or by mechanical polishing or scratching, which produce ridges, thicker film formation is again above the cell boundaries or ridges (in preparation). Further growth of the locally thicker material and the barrier layer, and a flattening of the initially ridged metal/film interface due to this more rapid growth at the ridges, are observed with continued anodising of an electropolished substrate (Fig 1*c*, *d*). Pores are formed next within preferred cells, resulting in the now markedly scalloped appearance of the metal/film interface (Fig. 1*e*, *f*). With further anodising, the width of the scalloped metal beneath the barrier layer increases, as does the diameter of the pore base in order to maintain a uniform barrier layer thickness (dependent on voltage), until the scalloped regions intersect and create the steady-state porous film morphology with

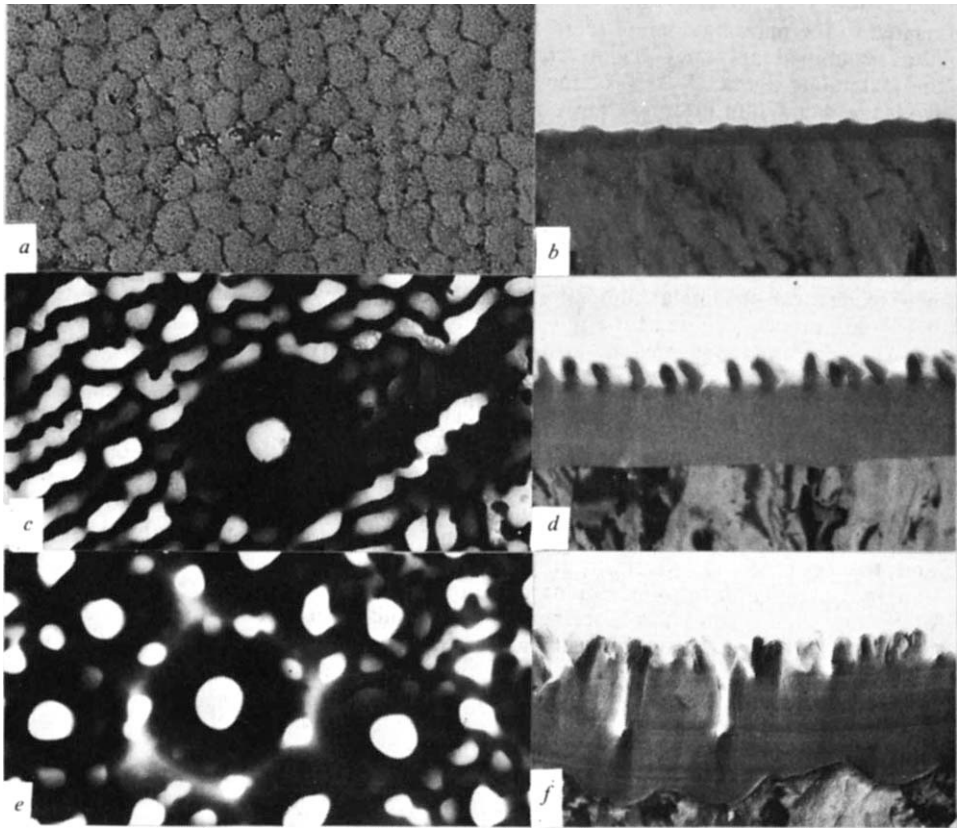

Fig. 1 Transmission electron micrographs of the films formed on electropolished aluminium for various times at 50A m^{-2} in 0.4 M phosphoric acid at 298 K. *a*, Stripped anodic film produced in 20 s, showing the non-uniform growth of the film with thicker material at the cell boundaries in an approximately hexagonal arrangement. *b*, Ultramicrotomed section of anodic film formed in 20 s, showing the scalloped nature of the metal/film interface and growth of thicker material above the ridges of metal. *c*, Stripped anodic film produced in 120 s, showing the elongated cellular appearance of the thicker film material (dependent on the metal grain orientation) and the onset of pore formation. *d*, Ultramicrotomed section of anodic film formed in 120 s, showing the thicker film material at the cell boundaries and the relatively flat metal/film interface. *e*, Stripped anodic film produced in 160 s, showing major pore development. *f*, Ultramicrotomed section of anodic film formed in 160 s, showing the scalloped metal/film interface beneath the developing pores. For *a–f* magnification × 80,000.

0028–0836/78/0272—0433$01.00

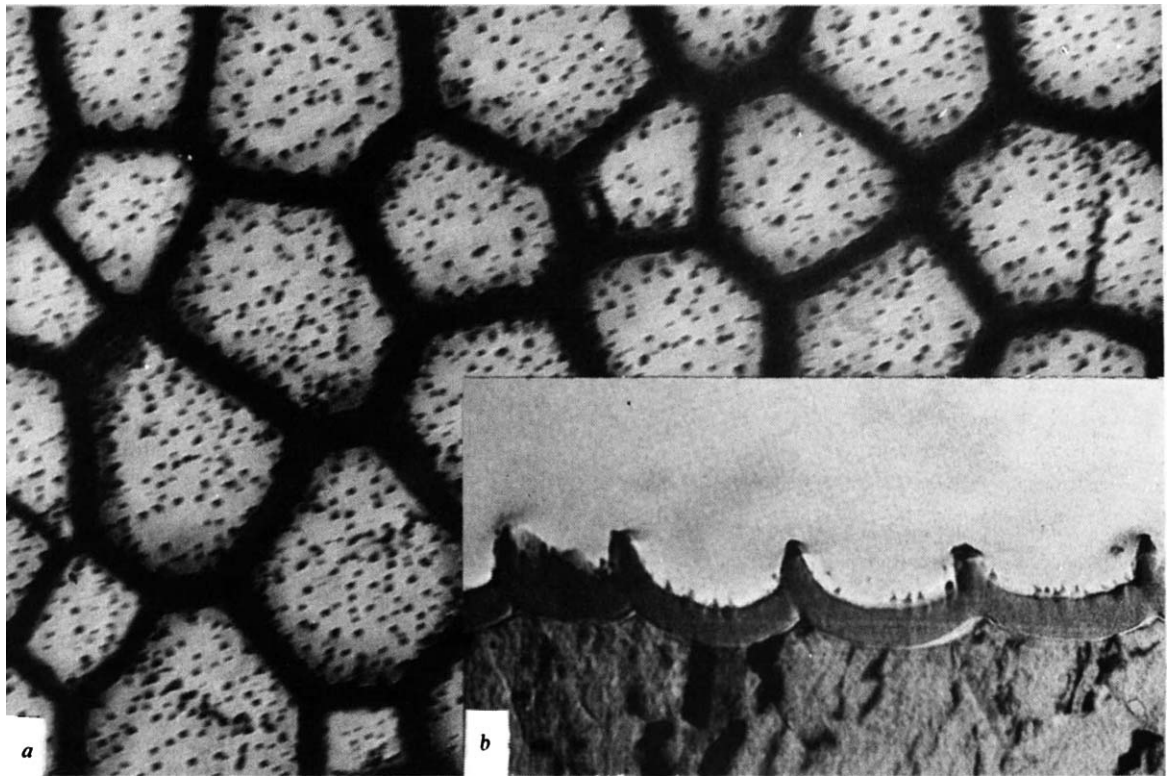

Fig. 2 Transmission electron micrographs of the film formed for 60 s on a preconditioned substrate at 50 A m^{-2} in 0.4 M phosphoric acid at 298 K. The preconditioned substrate was prepared by forming a steady-state porous film on the electropolished aluminium substrate in the above conditions for 10 min and removing the film in a mixture of boiling chromic acid–phosphoric acid. This produced an aluminium substrate with a cellular topography dependent on the steady-state anodising voltage (120 V). The nonhexagonal nature of the cells is related to the mechanism of porous anodic film formation. *a*, Stripped anodic film showing the development of thicker film material at the cell boundaries. The islands of locally thicker material within the cells have a population density of about 9×10^{14} m^{-2}. *b*, Ultramicrotomed section of a showing the development of thicker film material above the ridges of metal. × 80,000.

the major parameters dependent on the voltage.

In a parallel investigation secondary ion mass spectrometry was used to determine in-depth profiles of species related to the phosphate anion (data not shown). For all the films examined an inner region containing no phosphate and extending about 25–35% of the barrier layer thickness from the metal/film interface was observed. The results are in agreement with those determined previously for film growth in neutral phosphate solutions[6].

Consideration of our studies suggests a model for initial film growth involving two simultaneous processes. (1) Growth by ionic migration through an existing film occurs, that is, both Al^{3+} and OH^- and O^{2-} are mobile and form new oxide near the metal/film interface. (2) Growth by a deposition process occurs at the film/solution interface, that is, Al^{3+} ions not consumed in growth by ionic migration are ejected at this interface to form hydrated ions in solution. (Direct solid state film formation through combination of ejected Al^{3+} ions with OH^- and O^{2-} plus phosphate is not thought to be a major process in the anodising conditions used, as the outer layer of film material is considered to be differently textured.) Solid alumina can form by deprotonation of the hydrated Al^{3+} ions, aggregation and thence precipitation from initially colloidal hydrous alumina; many film-forming anions can influence the rate of precipitation[7]. The phosphate species can stabilise a fine colloidal particle size distribution and delay the precipitation of impure, hydrous alumina. It is proposed that deprotonation of hydrated Al^{3+} ions and aggregation with some phosphate ions produces negatively charged colloidal particles, held in solution through the influence of the incorporated phosphate, which are deposited under the field above the thickening phosphate-free layer to produce an outer layer of fine microcrystallites. Effective compaction of the deposited layer may occur by further deprotonation of the impure hydrated alumina by further reaction with some of the Al^{3+} ions ejected from the inner layer[8].

During anodising the field strength is greater across the compact inner layer than across the impure film material, which probably varies from solid near the inner layer to gel-like material towards the outer surface of the film. The ridges of metal apparently act as more favourable sites for film growth and localised deposition. This may arise from a larger impurity-derived flaw density in the vicinity of the ridges compared with the more uniform regions between the ridges; within the limits of resolution, cracking of the film above the ridges has not been observed. If the effective current density is greater at the ridges than over the larger scalloped metal area, more rapid growth of the inner layer, a faster rate of Al^{3+} ejection and more localised deposition are all expected. Conversely, the efficiency of deposition is reduced in the lower current density regions because of the slower rate of Al^{3+} ejection leading to instability of the hydrous oxide sol and greater loss of colloidal material to the aggressive solution. Thickening of the film at the protuberances concentrates the current and film growth further into the thinner film regions in an attempt to obtain a uniform film thickness and maintain a constant field strength. The distribution of cell sizes enables the current density within the cells to vary, allowing the film material within the smaller cells to thicken more efficiently than that within the larger cells where deposition is hindered because of the lower rate of Al^{3+} ion ejection. The larger cells then probably become the sites at which pores develop because Al^{3+} ions are lost to solution through the low effective rate of deposition; local scalloping of the metal beneath the

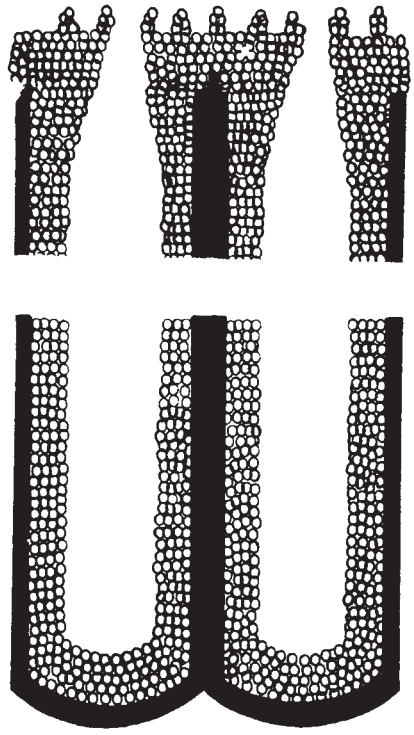

Fig. 3 Schematic diagram of the porous anodic film. The solid region represents the relatively pure alumina film material and the textured region depicts the microcrystalline film material with incorporated phosphate. The crystallites are not meant to be particularly regular and are probably of a size $\leqslant$ 2.5 nm. During anodising the field strength is greater across the compact inner layer than across the impure film material, which probably varies from solid near the inner layer to gel-like material in the vicinity of the pore base. The upper part of the diagram shows the appearance at the outer film/solution interface and the lower part of the diagram shows the steady-state morphology of the porous anodic film towards the metal/film interface.

barrier layer then proceeds in these preferred regions.

Steady-state film formation proceeds by steps (1) and (2) described above providing (3) transformation of the inner layer can occur. Transformation of the inner layer is also required to maintain the 2 : 1 ratio of phosphate-incorporated film material to relatively pure alumina in the barrier layer. The relative ease of transformation governs the steady-state anodising rate; this process may be identified as field-assisted dissolution or interface potential-assisted dissolution[9], which is thermally enhanced. The H^+ and phosphate species move in the intercrystallite regions of the outer layer; there is no phosphate mobility under the field in the inner layer.

Figure 3 is a schematic diagram of the porous anodic film, showing the relatively pure alumina region and the phosphate-incorporated film material.

We thank the SRC and Howson-Algraphy Ltd for financial support.

G. E. THOMPSON
R. C. FURNEAUX
G. C. WOOD
J. A. RICHARDSON
J. S. GOODE

Corrosion and Protection Centre,
University of Manchester Institute of Science and Technology,
PO Box 88,
Manchester, UK

Received 17 October 1977; accepted 3 February 1978.

1. Hoar, T. P. & Mott, N. F. *J. Phys. Chem. Solids* **9**, 97–99 (1959).
2. O'Sullivan, J. P. & Wood, G. C. *Proc. R. Soc.* **A317**, 511–543 (1970).
3. Siejka, J. & Ortega, C. *J. electrochem. Soc.* **6**, 883–891 (1977).
4. Thompson, G. E., Furneaux, R. C. & Wood, G. C. *Trans. Inst. Metal Finishing* **55**, 117–128 (1977).
5. Thompson, G. E., Furneaux, R. C. & Wood, G. C. *Corros. Sci.* (in the press).
6. Abd Rabbo, M. F., Richardson, J. A. & Wood, G. C. *Corros. Sci.* **16**, 689–702 (1976).
7. Matijevic, E., Bell, A., Brace, R. & McFadyen, P. *J. electrochem. Soc.* **120**, 893–899 (1973).
8. Alwitt, R. S. in *Oxdies and Oxide Films* **2** (eds Diggle, J. W. & Vijh, A. J.) 169–284 (Dekker, New York, 1976).
9. Diggle, J. W. in *Oxides and Oxide Films* **2** (ed. Diggle, J. W.) 281–386 (Dekker, New York, 1973).

Formation of films in hydrolysing ferric chloride solutions

FRYER *et al.*[1,2] have postulated that two-dimensional polymeric structures may be formed in solution when metal-ion salts undergo self-hydrolysis before the precipitation of some hydrated crystalline oxides such as α FeO.OH, β FeO.OH, and $V_2O_5.H_2O$. They reported that these structures or films can only be seen by spraying a hydrolysing solution onto a mesh of asbestos fibres when the film appears suspended between the asbestos fibres supported on the copper grid. We describe here how we have repeated this work using 0.01 M $FeCl_3$ with both an asbestos mesh and a holey carbon support film (Fig. 1) and have obtained similar results. The films we have seen have large dimensions, of the order of several microns and of varying thickness depending on the drop size of the spray and the size of the mesh or hole. Assuming that the minimum thickness of the film is about the same as that of the partially hydrolysed spherical polymers seen by Murphy *et al.*[3], that is, 10–50 Å then the equivalent spherical diameter (e.s.d.) of the films would be about 3,000 Å. Our observations of the films suggest that they can be much thicker than this.

If films of this order of size are actually present in these solutions, then it should be easy to centrifuge them out of the hydrolysing solution. A sample of the 0.01 M solution of $FeCl_3$ (pH 2.4) was centrifuged for 1 h at 60,000 r.p.m. in a L2.65B Spinco centrifuge using a TY65 head. The supernatant from the top half of the tube was sampled and examined. The same film as that seen in the original uncentrifuged sample was observed (Fig. 1). The solution collected from the bottom of the tube did not show a higher level of film, but there was a small amount of β FeO.OH depending on the age of the solution. The conditions of centrifugation should have sent to the bottom of the tube all particles with an e.s.d. greater than about 60 Å. These results suggested that the films were artefacts of the method of examination. This was confirmed by a further experiment in which $FeCl_3$ (0.01 M) was hydrolysed in H_2O (pH

Fig. 1 0.01 M $FeCl_3$ solution (pH 2.4) in the early stages (2 h) sprayed onto a holey carbon support film showing a fine grained film covering the holes in the carbon film. Scale bar, 1 μm.

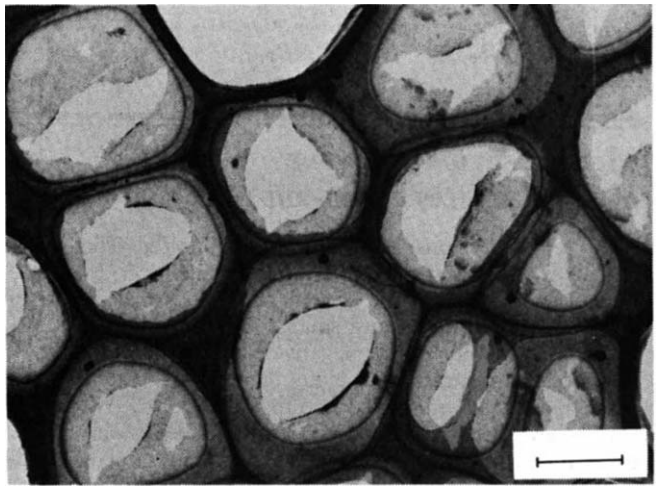

0028–0836/78/0272—0435$01.00